Modeling the Postcure Regime of Ablative Composite Materials

Zivorad R. Lazic* and Jova P. Hrabar†
Military Technical Institute, Belgrade, Yugoslavia

Ablative polymer materials based on phenol-formaldehyde resins regardless of reinforcement or filler are the most frequently processed by compression molding at increased temperature. The prepared material is then postcured. The postcured process is optimized in time and temperature by the introduction of a nongradient optimization technique called Sequential Simplex Design (SSD). Once the local optimum is reached, mathematical modeling of the real optimum is obtained by using the Simplex-Sum Rotatable Design (SSRD) of the second order. The obtained regression model is adequate at 99% confidence level. The postcure regime does not depend on duration, but on the postcure temperature.

Introduction

ABLATIVE polymer materials based on phenol-formaldehyde resins, regardless of reinforcement or filler, are the most frequently compression molded at elevated temperature and postcured upon removal from the mold. The process in the mold lasts minutes, while the postcure process takes tens of hours. The aim of the postcure process is to achieve the maximum degree of curing by minimum use of the compression mold. The optimization of the postcure time and temperature is made by the application of a nongradient optimization technique called Sequential Simplex Design (SSD). The local optimum is reached by the SSD technique, after which the mathematical modeling of the real optimum is obtained by using Simplex-Sum Rotatable Design (SSRD) technique.

Thermal Degradation of Phenol-formaldehyde Resins in the Ablation Process

Ablation cooling, or simply ablation, denotes the process of thermal protection of surface material, which is exposed to the stream of a hot gas, through the process of a "sacrificial loss" of the same.

Ablative polymer materials dissipate the imposed heat flux by four principal mechanisms[1]:

1) Stored energy which produces a temperature rise in the ablative material;

2) Latent heat of physical changes such as depolymerization, melting, vaporization, and sublimation;

3) Radiant energy losses from the high temperature ablating surface;

4) Transpiration cooling by gaseous decomposition products injected into the boundary layer. These gases thicken the boundary layer and reduce the rate of heat transfer to the ablating surface.

One of the most important aspects of ablative polymer materials is the process of binder depolymerization, in which considerable amount of externally imposed heat can be absorbed.

Phenol-formaldehyde resins of resole type is the most frequently used binder in ablative composite materials for thermal protection. There are papers dealing with all the important aspects of heat decomposition of phenol resins such as the mechanism and decomposition products, heat effects, and kinetics. Although a typical cross-linked resin phenolics are ill defined, their wide application in the ablation processes promoted intensive investigations.

In phenol-formaldehyde resins, neither the onset nor the end of pyrolysis is well defined, as shown by TGA curves in literature.[2] Some weight losses occur around 300°C, but the actual pyrolysis starts nearer to 400°C. The maximum weight loss rate occurs around 500°C, and pyrolysis is considered mostly complete by about 900°C. Approximately one half of the material volatizes and one half is left as a carbonaceous residue or char.[2]

For a long period of time, it has been considered that the degradation of phenol-formaldehyde resins commences with the rupture of the bond between the methylene group and aromatic ring. A different mechanism was postulated recently by Jackson and Conley,[2] as a result of an experimental observation that the primary degradation route was the same regardless of whether the pyrolysis was conducted in air, argon, or nitrogen. The degradation was always oxidative, the resin apparently providing its own oxygen atoms from the hydroxyl groups, Fig. 1.

This proposed mechanism seems plausible. The value of the activation energy for the early state of decomposition is

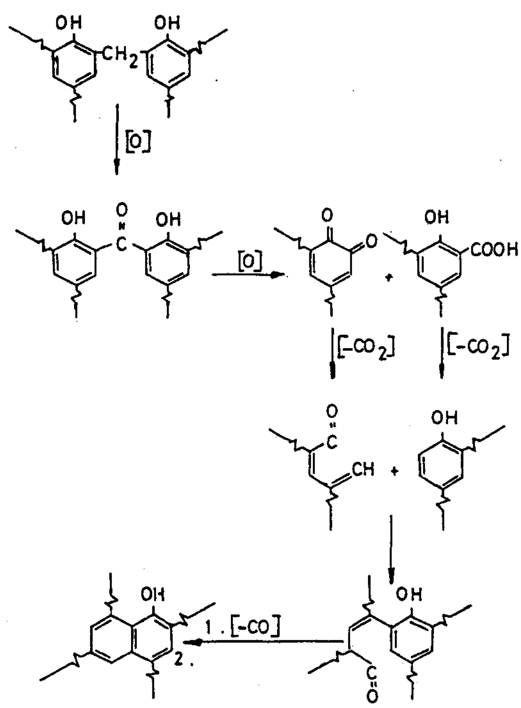

Fig. 1 Degradation mechanism.

Received Aug. 17, 1989; revision received Aug. 3, 1990; accepted for publication Aug. 3, 1990.

*Director of Engineering.

†Chemical Engineer.

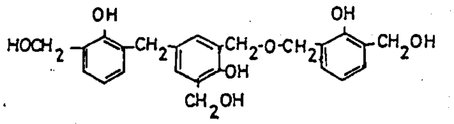

Fig. 2 Resol structural formula.

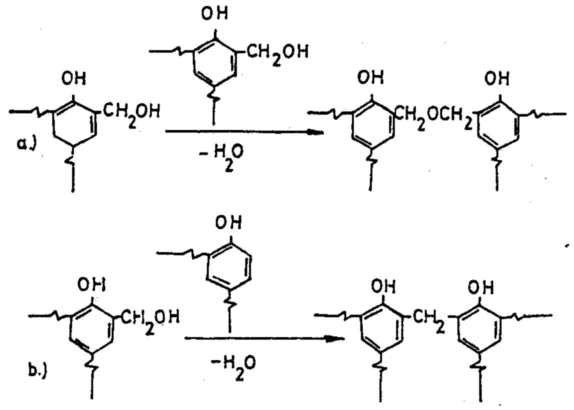

Fig. 3 Curing mechanism.

approximately 75.4 kJ/mol, while the apparent activation energy of the oxidation of the methylene bridge was found to be the order of 79.5 kJ/mol. This agreement corroborates the initial steps of the mechanism. Contrary to the finding of other workers,[2] the proposed mechanism does not predict the evolution of hydrogen. However, the analytical procedures differed. All this indicates that one can only disapprove a possible reaction mechanism, but never prove it.[2]

Regardless of the fact that the degradation of phenol-formaldehyde resins starts with the rupture of the bond between the methylene group and an aromatic ring, or by the oxidation of methylene group, however, these reactions do require an activation energy.

Since the methylene group between the aromatic rings is formed in the process of polycondensation of phenol-formaldehyde resins, it is obvious that greater amount of energy in the degradation process will be absorbed if there are more methylene groups between the aromatic rings per unit volume.

Heating of resoles, polynuclear polyalcohols of general formula, Fig. 2, will result in cross-linking via the uncondensed methylol groups. In general, cross-linking at temperatures below 160°C occurs by condensation of phenolmethylol-phenolmethylol, or phenol- methylol-phenol, as seen in Fig. 3.

The Approach to Solving the Problem

Because of the difficulties in evaluating the degradation mechanism of phenol-formaldehyde resins and activation energies, an indirect approach to determine thermally the most stable structures was made. If it is accepted that the highest quantity of heat is taken up by the activation process of oxidation of methylene groups in the degradation process, then the total amount of energy absorbed would be proportional to the number of available methylene groups between the phenol rings, i.e., the degree of cross-linking.

The structure of the polymer binder is determined by this reasoning, but not the activation energy of the decomposition process. Then, through the structure of polymer, its thermal stability can be evaluated.

Lately, data from dynamic mechanical spectra are used in many papers for evaluation of viscoelastic properties of polymer materials as well as composites.[3-7] The polymer structure, i.e., the degree of cross-linking, in those papers was analyzed by the second-order transition temperature. The

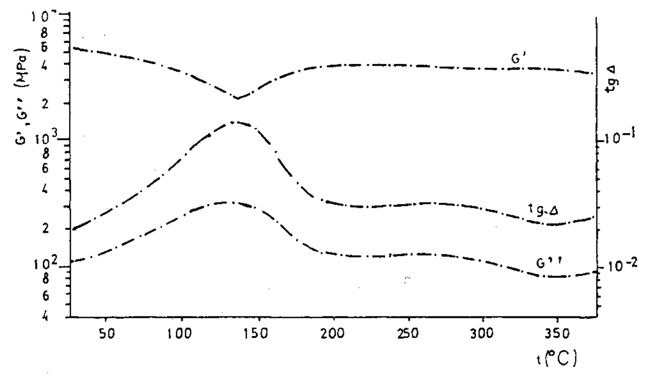

Fig. 4 Measurement of reological properties.

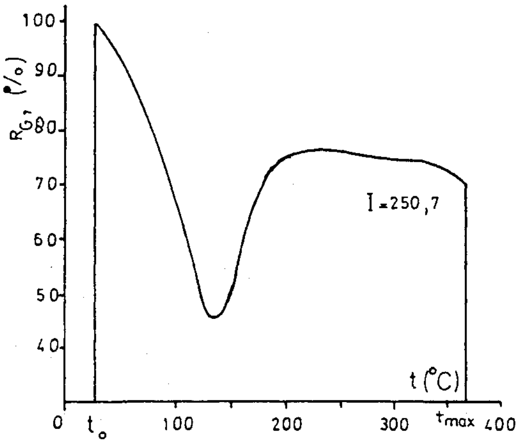

Fig. 5 $R_{G'}$ versus temperature.

techniques that were used have sufficient resolution to separate the influence of the structure of a binder component from the reinforcement effect in a composite material.

The aim of this work was to achieve better resolution of the cross-linking degree and optimization of the postcure regime for thermal protection materials.

The data for shear storage modulus G' vs temperature of a postcured composite material, shown in Fig. 4, were used to start the determination of the degree of cross-linking. Analogous to the data recording for the mass loss in TGA, the modulus "loss" was calculated for every test temperature. The modulus loss, or relative change of storage modulus with temperature is given as

$$R_{G'} = \frac{G'_t}{G'_{26^\circ C}} \tag{1}$$

where $R_{G'}$ is the relative change of storage modulus (Eq. 1); G'_t is the shear storage modulus at test temperature t [MPa]; $G'_{26^\circ C}$ is the shear storage modulus at initial temperature of 26°C [MPa].

The storage modulus with constant strain rate (frequency), expressed as a function of temperature, yields a measure of elasticity of the material for every test temperature. The storage modulus is dependent on polymer structure.

The difference in absolute moduli values which can be assigned to any parameter of nonhomogeneity of composite material is eliminated by applying the relative change of modulus, thus, emphasizing the changes in the binder component. If relative changes of moduli are expressed as a function of temperature, Fig. 5, a continuous curve is obtained over the entire temperature interval. Thus, the second-order transition temperature behavior of the material can be followed over a certain temperature interval, rather than over only a few points.

For thermoprotective polymer composite materials based on phenol-formaldehyde resins, considering the role of methylene groups between the phenolic rings, the most desirable effect would be to obtain a maximum possible overall cross-linking density. This effect causes the smallest change of modulus with temperature.

It is necessary to define the parameter that would characterize the above phenomenon. The relative change of the shear storage modulus as a function of temperature can be expressed mathematically as

$$R_{G'} = f(t) \tag{2}$$

It is required that the area under function $R_{G'}$ over a given temperature interval, has the highest possible value. The lower limit is the initial test temperature t_0 and the upper limit is the final test temperature:

$$I = \int_{t0}^{t\max} R_{G'} \mathrm{d}t \tag{3}$$

The integral value (Eq. 3) is graphically calculated from the experimental storage modulus vs temperature for every different postcure regime of phenol-formaldehyde resins.

Experiment

Experimental Procedure

The aim of the experimental work was to establish the optimum postcure regime for the selected ablative phenol-formaldehyde resin of resole type by the design of an experiment for previously defined thermoprotective composite material.

The tests were conducted on the composite with chopped "E" type glass fibers, impregnated with commercial type of phenol-formaldehyderesin "Borofen DX-26" ("DONIT" Yugoslavia). The weight ratio of resin to glass fibers in the composite was 40 to 60. Compression molding of the material was made using specimen mold, according to DIN 53470.

The molding conditions were: 1) molding temperature 150°C; 2) specific molding pressure 20 MPa; and 3) molding time for specimen thickness 3 mm, 20 min.

The postcure of the specimen, in accordance with Table 4, was made in the forced air oven, without additional loading. Specimens were placed into a preheated oven, and after the postcure time has elapsed, allowed to cool in an oven at the cooling rate of 10°C per 10 min down to 30–40°C.

Dynamic shear properties were measured with the mechanical spectrometer "RMS-605," from "Rheometrics," on specimens approximately 65 × 12 × 3 mm, at the strain rate of 6.28 s^{-1} (1 Hz) and strain of 0.1%. The temperature was varied from 26°C to 375°C, in steps of 15°C, and a thermal soak time of 3 min. at each measurement. The obtained shear properties are shown in Fig. 4. The values of R_G are calculated for every temperature using Eq. (1), and the function given by Eq. (2) is obtained, see Fig. 5. The graphical value of the integral of the function (Eq. 2) in a certain temperature interval is determined next and represents the system response (Y). See Fig. 4 and Fig. 5.

Design of Experiment

Sequential Simplex Design (SSD)

The method of SSD in the design of experiment is a non-gradient optimization technique in a polydimensional factor space. In contrast to gradient optimization techniques, this methodology does not require mathematical modeling for the investigated phenomenon.

The advantages of the SSD are: 1) Application of the design of experiments in the extreme, with large amount of scatter and, 2) Application of the design of experiments in the extreme, where qualitative factors are included as well.

Simplex designs were first introduced in 1962[8] and this methodology has been constantly upgraded.[9–12]

The Simplex is a simple geometrical form created by (k + 1) independent vertices in a k-factor space, in which the experimental, or factor space, is defined by the number of factors, variables.

The number of points, i.e., vertices, in a simplex form is the minimum and for k-factors it is $k + 1$. A regular k-simplex is designed as a set of $k + 1$ equidistant vertices.

The simplex is regular if the distances between the simplex vertices are identical. However, by respective mathematical transformations any simplex can be turned regular. In a plane (two-factor experiment), a regular simplex has the form of an equilateral triangle. In three dimensions, i.e., a three-factor space, the simplex is represented by tetrahedron. Any simplex can be transformed into a new one by adding one point and rejecting a vertex from the starting simplex. This is the property of the simplex design that is used to shift towards the optimum.

The shifting towards the optimum is stepwise, by successive rejection of the vertex with poorest response and with a new vertex constructed as a mirror reflection of the rejected vertex. In the next step the experiment is carried out in the new vertex, and again the vertex with poorest response is rejected and the procedure repeated.

The strategy of simplex optimization consists of: a) designing the starting simplex; b) defining the coordinates of a new vertex; c) defining the proper stopping time.

Beside these three tasks, it is important to know how to pass from SSD to the Second-Order Design to define the optimum area.

The first task in the SSD is to design the matrix for the starting simplex with the coordinates of the given experimental points (vertices). Different orientations of the starting simplex are possible with respect to the system of coordinates. Most frequently, the center of the simplex is the origin of coordinates, with an edge of unity. As a rule, the simplex is oriented to the space factor so that the vertex b_{k+1} lies on axis x_k, and other vertices are symmetrical to the coordinate axes. The simplexes of such a design are shown in Figs. 6 and 7. According to these figures, the coordinates of the vertices

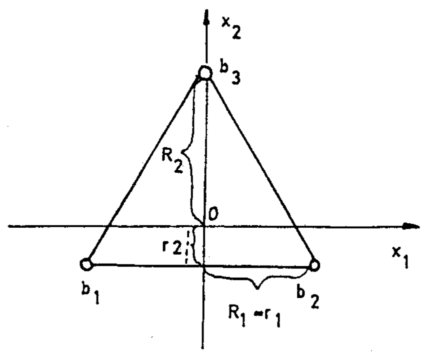

Fig. 6 Orientation of two-dimensional simplex.

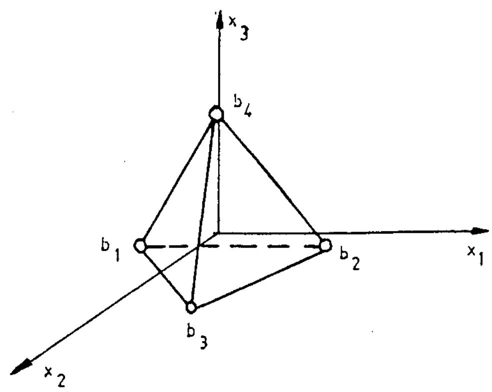

Fig. 7 Orientation of three-dimensional simplex.

Table 1 Design points for k-factors

No.	Coded factors									Y_u
	$X_1\|1\|$	$X_2\|1\|$	$X_3\|1\|$	$X_4\|1\|$	$X_5\|1\|$	$X_6\|1\|$	$X_7\|1\|$	···	X_k^*	|°C|
1	−0.500	−0.289	−0.204	−0.158	−0.129	−0.109	−0.0945	···	$1/[2k(k+1)]^{0.5}$	y_1
2	0.500	−0.289	−0.204	−0.158	−0.129	−0.109	−0.0945	···		y_2
3	0	0.578	−0.204	−0.158	−0.129	−0.109	−0.0945	···		y_3
4	0	0	0.612	−0.158	−0.129	−0.109	−0.0945	···		y_4
5	0	0	0	0.632	−0.129	−0.109	−0.0945	···		y_5
6	0	0	0	0	0.645	−0.109	−0.0945	···		y_6
7	0	0	0	0	0	0.654	−0.0945	···	$[k/2(k+1)]^{0.5}$	y_7
8	0	0	0	0	0	0	0.6620	···		y_8
·	·	·	·	·	·	·	·	···		·
k + 1	0	0	0	0	0	0	0	···		y_{k+1}

k-Number of factors.

Table 2 The optimum matrix $k = 2$ of the starting simplex

Design points	Coded factors	
	$X_1\|1\|$	$X_2\|1\|$
1	−0.865	−0.500
2	0.865	−0.500
3	0.000	1.000

are equal to the radii of the inscribed (r_k) and circumscribed sphere (R_k) of k-dimensional simplex. For the two-dimensional simplex the radii r_2 and R_2 has to be known.

For the selected simplex orientations over the factor space, the vertex coordinates could be determined from the following matrix:

$$\left\| \begin{matrix} -r_1 & -r_2 & -r_3 & \cdots & -r_{k-1} & -r_k \\ -R_1 & -r_2 & -r_3 & \cdots & -r_{k-1} & -r_k \\ 0 & R_2 & -r_3 & \cdots & -r_{k-1} & -r_k \\ \cdot & \cdot & \cdot & \cdots & \cdot & \cdot \\ 0 & 0 & 0 & \cdots & R_{k-1} & -r_k \\ 0 & 0 & 0 & \cdots & 0 & R_k \end{matrix} \right\|$$

The radii of the inscribed (r_k) and circumscribed (R_k) spheres for a k-dimensional simplex are

$$r_k = \frac{1}{[2k(k+1)]^{0.5}}; \quad R_k = \left(\frac{k}{2(k+1)}\right)^{0.5} \tag{4}$$

Examples:

For $k = 0$, dimensional simplex is reduced to a point, in the center of the coordinate system.

For $k = 1$, regular simplex is a straight line with two vertices (ends), lying on axis x_1 with coordinates +0.500 and −0.500.

For $k = 2$, coordinates of the simplex vertex can be drawn graphically or calculated from Eq. (4).

As seen in Fig. 8, the three vertices of this simplex have the following coordinates:

$$b_1(-0.500;\ -0.289);\ b_2(+0.500;\ -0.289);\ b_3(0;\ 0.578)$$

For $k = 7$, in conformity with Eq. (4), the following is obtained

$$r_7 = \frac{1}{(2.7(7+1))^{0.5}} = 0.0945;\ R_7 = \left(\frac{7}{2(7+1)}\right)^{0.5} = 0.662$$

For a defined number of factors, the coordinates of the experimental points in a specific problem are given in Table

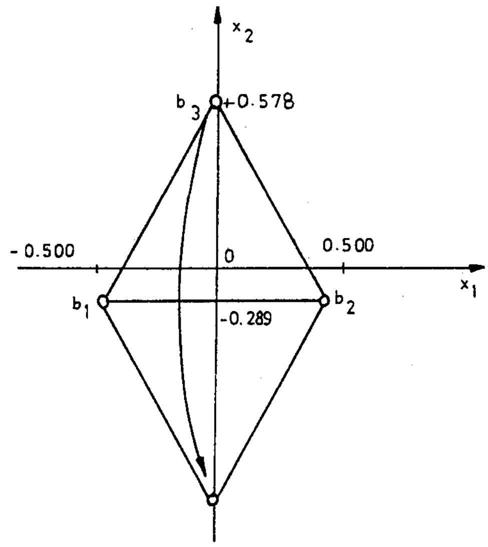

Fig. 8 Coordinates of two-dimensional simplex.

1. A matrix transformation is necessary to reach the optimum of the design of the experiment.

It is known that the design of an experiment is considered optimal when the following conditions are fulfilled:

1) The matrix of the design of experiment is orthogonal;

2) Independent variables are symmetrical with respect to the center of the experiment; and

3) The sum of squares of elements of matrix collumns are equal.

The matrix in Table 1 does not fulfill only the third condition. For the two-dimensional simplex ($k = 2$), the values in columns X_1 and X_2 (Table 1) are divided by the highest value of the element, which is 0.578. Table 2 is formed with this transformation.

When the Simplex matrix is setup along with coded factor values, it is necessary to pass to the real matrix with real values of factors, while taking into account the intervals of factor variation and coordinates of the center of experiment. The general equation for the transformation from coded to real values is

$$X_k = \frac{x_k - x_{k_0}}{\Delta x_k} \tag{5}$$

where X_k = coded factors[8]; x_k = real factors; x_{k_0} = real factors in the center of experiment; and Δx_k = unit or interval of factor variation.

The simplex is advanced over the factor space by rejecting the point that yields the poorest response and defines the coordinates of the next vertex, which is a mirror reflection of the rejected vertex:

$$X_{ij}^{(k+2)} = \frac{2}{k}\sum_{i=1}^{k} X_{ij} - X_{ij}^{*} \tag{6}$$

where $X_{ij}^{(k+2)}$ = coordinate of the added vertex; X_{ij}^{*} = coordinate of the vertex with poorest response; $2/k \sum_{i=1}^{k} X_{ij}$ = average of coordinates of vertices except the rejected one; k = number of factors; i current factor of coordinate; j current number of design points; and $(k + 2)$ = next number of design points.

Simplex-Sum Rotatable Design of the Second Order (SSRD)

The space of the local optimum is very often determined in conducting the SSD. In such a situation, the experimenters wishes to make a mathematical model of the optimum. Since the optimum is the extreme value of the response, in principle it could be approximated with the Second-Order Model. In the design of experiments the Second-Order Model is assessed by the Second-Order Design of Experiments. The most common designs of the second order are orthogonal and centrally composite rotatable.[13]

The noncomposite design, such as the SSRD of hexagon type ($k = 2$) with central points (Fig. 9), is used for solving the aim of this work. The SSRD is the smallest rotatable design of the second order.[14] It is easily split up into two blocks having three vertices of a triangle, plus $n_0/2$ central points. A characteristic of this design is that the factor x_1 requires five levels of variations. This property is very important since in practice the number of variations is frequently restricted.

Figure 9 shows that a = 0.5 (2a = 1), or 3a = 0.87, so that coded levels could be written as follows: −1; −0.5; 0; +0.5; +1 for x_1 and −0.87; 0; +0.87 for x_2. The matrix for the design of an experiment is presented in Table 3. The transformation from coded to real factors is carried out by Eq. (5).

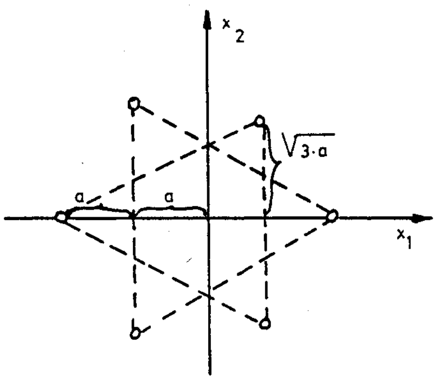

Fig. 9 SSRD of a hexagon type.

Table 3 SSRD matrix

Design points	Coded factors					Response
	$X_1\|1\|$	$X_2\|1\|$	X_1X_2	X_1^2	X_2^2	$y\|°C\|$
1	−	0	0	+	0	y_1
2	+	0	0	+	0	y_2
3	0.5	0.87	0.43	0.25	0.75	y_3
4	0.5	−0.87	−0.43	0.25	0.75	y_4
5	−0.5	0.87	−0.43	0.25	0.75	y_5
6	−0.5	−0.87	0.43	0.25	0.75	y_6
7	0	0	0	0	0	y_7
8	0	0	0	0	0	y_8
9	0	0	0	0	0	y_9
10	0	0	0	0	0	y_{10}

The SSRD by its nature, according to Box and Behnken[15] consists of two simplexes with its respective number of central points. This can be split up into two orthogonal blocks to eventually allow time effect analysis of the experimental results, see Table 3.

Following the quoted paper,[15] the SSRD does not fully satisfy the conditions of orthogonality and rotatability. Therefore, calculations of regression coefficients corrections must be introduced for the rotatable but not orthogonal blocks or rotatable designs.

Discussion

To confirm the definition of experimental objective the real factors were:

$$x_1\ (°C) = \text{temperature}$$

$$x_2\ (h) = \text{time}$$

The centerpoint of the design or zero level of factors was determined from experience and previous knowledge

$$x_{10} = 120\ (°C)$$

$$x_{20} = 10\ (h)$$

From estimates of the precision of the equipment we use

$$\Delta x_1 = 40\ (°C)$$

$$\Delta x_2 = 8\ (h)$$

The starting Simplex was set (Table 2) when the above values were defined following the theory of the SSD. The design matrix of the starting Simplex is turned into a real matrix using Eq. (2). The matrix of design together with the real matrix and response values is shown in Table 4.

Design Points 1 to 3 were carried out according to Table 4. Those points are the vertices of the starting simplex. From the results obtained, it is evident that the response of the first point has the minimum degree of cross-linking. Thus, its vertex is rejected. Simplex optimization and conditions for performing the test are determined to be the mirror reflection of test No. 1, according to Eq. (3)

$$x_1^{(2+2)} = \frac{2}{2}\sum_{i=1}^{2} (0.865 + 0.000) - (-0.865) \Rightarrow x_1^4 = 1.730$$

$$x_2^{(2+2)} = \frac{2}{2}\sum_{i=1}^{2} (0.500 + 1.000) - (-0.500) \Rightarrow x_2^4 = 1.000$$

The real values of the factors in the design point No. 4 area

$$x_1^4 = x_{10} + x_1^4\Delta x_1 = 120 + 1.730\ 40 = 189\ (°C)$$

$$x_2^4 = x_{20} + x_2^4\Delta x_2 = 10 + 1.000\ 8.0 = 18\ (h)$$

The Design Point 4 was performed and the value of the response y_4 = 303 (°C) is obtained. If this response is compared with the two previous vertices (y_2 = 278 (°C); y_3 = 281 (°C)), it is found that the poorest response is at Design Point 2. Following the theory of SSD, the Design Point No. 2 is rejected and conditions for Design Point 5 are defined. The procedure for defining the next design point conditions is identical to the previous one. The test conditions for the Design Point 5 and all the other design points are given in Table 4. The geometric interpretation of the simplex proceeding from Table 4 is shown in Fig. 10.

It is evident from Fig. 10 that the simplex was "cycled." The values obtained for cycled simplex could be turned into the SSRD design of the second order with minimum additional

Table 4 Design matrix and real matrix

Design Points*	Design matrix $X_1\|1\|$	$X_2\|1\|$	Real matrix $X_1\|°C\|$	$X_2\|h\|$	Response $y\|°C\|$	Remarks
1	−0.865	−0.500	85.0	6.0	251	
2	+0.865	−0.500	155.0	6.0	278	Starting
3	0.000	1.000	120.0	18.0	281	Simplex
4	1.730	1.000	189.0	18.0	303	
5	0.865	2.500	155.0	30.0	298	
6	2.595	2.500	224.0	30.0	302	Proceeding
7	3.460	1.000	258.0	18.0	307	towards
8	2.595	−0.500	324.0	6.0	—	optimum

*Design point = Postcure conditions (X_1; X_2).

Table 5 SSRD matrix

No.	Design matrix X_1	X_2	X_1X_2	X_1^2	X_1^2	Real matrix X_1 (°C)	X_2 (h)	Response y_u (°C)	$\hat{y}_u$	$(y_u - \hat{y}_u)^2$
1	−	0	0	+	0	120	18	281	280	1.0
2	+	0	0	+	0	258	18	307	308	1.0
3	0.5	0.87	0.43	0.25	0.75	224	30	302	301	1.0
4*	0.5	−0.87	−0.43	0.25	0.75	224	6	305	301	16.0
5	−0.5	0.87	−0.43	0.25	0.75	155	30	298	287	121.0
6	−0.5	−0.87	0.43	0.25	0.75	155	6	278	287	81.0
7*	0	0	0	0	0	189	18	301	294	
8*	0	0	0	0	0	189	18	310	294	
9*	0	0	0	0	0	189	18	306	294	
10*	0	0	0	0	0	189	18	306	294	

*The design points performed in addition to those of Table 4. All the other design points are illustrated in Table 4.

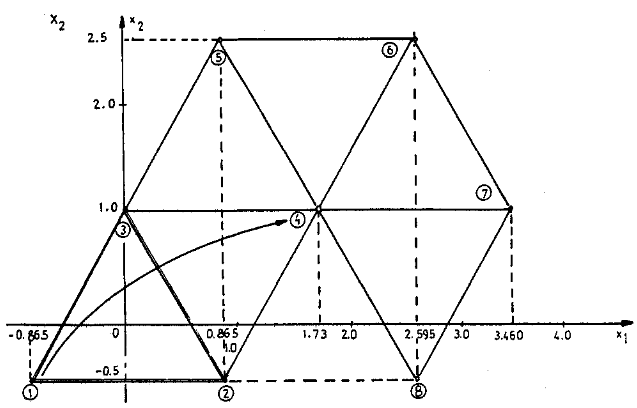

Fig. 10 Movement of simplex towards optimum.

points. This design with data computed enables mathematical modeling of response as a function of investigated factors.

When the center of experiment is shifted to the Design Point 4 and the interval of factor variations is transformed to

$$x_{10} = 189\ (°C) \qquad x_{20} = 18\ (h)$$

$$x_{10} = 69\ (°C) \qquad \Delta x_{20} = 8\ (h)$$

only one design point is to be carried out in Point 4 and four tests in the new center of experiment (x_{10} = 189°C and x_{20} = 18 h), see Table 5.

After conducting tests in the above specified points, complete results were obtained for the SSRD which are shown in Table 5.

Conclusion

Following the theory of SSRD, the optimal postcure regime for phenol-formaldehyde resin was defined. The experiments were conducted with the compression molded composite based on glass-fibers impregnated with phenol-formaldehyde resin. The aim was to achieve the maximum cross-linking degree of the resin in the composite.

The method for calculating the graphic value of the integral of relative change of the shear modulus function in the specified temperature is discussed. The method is based on the results obtained for the shear storage modulus as a function of temperature.

The SSRD results were used for computing regression coefficients. The obtained regression model, with .01 confidence level, was

$$y = 294 + \frac{14(x_1 - 189)}{69}$$

where x_1 = the postcure temperature and y = the graphic value of the integral of relative change of function of the shear storage modulus over the temperature interval from 26 to 273°C.

The model is adequate in the following space factor: a) the interval of the postcure temperature from 120 to 258°C and b) the interval of the postcure duration from 10 to 26 h.

The postcure regime, according to the regression model, does not depend on the duration, but only on the postcure temperature.

References

[1]Jellinek, H. H. G., *Aspects of Degradation and Stabilization of Polymers*, Elsevier Scientific Publishing, Amsterdam, 1978, p. 528.

[2]Landel, R. F., and Rembaum, A., *Chemistry in Space Research*, American Elsevier Publishing, New York, 1972, p. 279.

[3]Kinjo, N., Numata, S. I., and Koyama, T., "Synthesis and Viscoelastic Properties of New Thermosetting Resins Having Isocyanate and Oxazolidone Ring in Their Molecular Structure," *Journal of Applied Polymer Science*, Vol. 18, 1983, pp. 1729–1741.

[4]Drzewinski, M., and Macknight, W. J., "Structure and Properties of Sulphonated Polysulfone Jonomers," *Journal of Applied Polymer Science*, Vol. 30, 1985, pp. 4753–4770.

[5]Botta, A., de Candia, F., and Palumbo, R., "Glass Transition in Aliphatic Polyamides," *Journal of Applied Polymer Science*, Vol. 30, 1985, pp. 4753–4770.

[6]Shimbo, M., Ochi, M., and Jesako, H., "Mechanical Relaxation Mechanism of Epoxide Resins Cured with Acid Anhidrides," *Journal*

of Polymer Science (Polymer Physics Edition), Vol. 22, 1984, pp. 1461–1470.

[7]Kolaric, J., "Dynamic Relaxation Behavior of Copolymers of n-Butil Acrylate and of 2-Hydroxyethyl Methacrylate with Ethyl Acrylate, n-Butil Acrylate and Dodecyl Methacrylate, *Journal of Polymer Science (Polymer Physics Edition)*, Vol. 21, 1983, pp. 2445–2451.

[8]Spendley, W., Hext, G. R., and Himswort, F. R., "Sequential Applications of Simplex Designs in Optimization and Evolutionary Operation," *Technometrics*, Vol. 4, No. 4, 1962, p. 441.

[9]Tihomirov, V. B., *Matematiceskie metody planirovanija eksperimenta pri izuceniji netkanih materijalov*, Lehkaja Industrija, Moskva, 1968.

[10]Krug, G. K., *Matematiceskie opisanije i optimizacija mnogofaktornyh procesov*, Trudy, Moskva, 1966.

[11]Krug, G. K., *Problemy planirovanija eksperimenata*, Nauka, Moskva, 1969.

[12]Krug, G. K., *Planirovanije eksperimenata*, Nauka, Moskva, 1966.

[13]Nalimov, V. V., and Cernova, N. A., *Statisticeskie metody planirovanija ekstremalnyh eksperimentov*, Nauka, Moskva, 1965.

[14]Box, G. E. P., and Wilson, K. B. J., "On the Experimental Attainment of Optimum Conditions," *Royal Statistical Society*, Vol. 13, No. 5, 1951.

[15]Box, G. E. P., and Behnken, D. W., "Simplex-Sum Designs: A Class of Second Order Rotatable Designs Derivable from those of First Order," *Technometrics*, Vol. 2, No. 4, 1960, pp. 838–864.